THE ASTROPHYSICAL JOURNAL, 229:624–641, 1979 April 15

MERIDIONAL CIRCULATION AND CNO ANOMALIES IN RED GIANT STARS

ALLEN V. SWEIGART
Laboratory for Astronomy and Solar Physics, NASA Goddard Space Flight Center
AND
JOHN G. MENGEL
Yale University
Received 1978 October 9; accepted 1978 November 1

ABSTRACT

The possibility that meridional circulation due to internal rotation might lead to the mixing of CNO-processed material from the vicinity of the hydrogen shell into the envelope of a red giant star has been investigated and found to be generally consistent with the observational data on weak G band and CN-strong stars and on stars with low $^{12}C/^{13}C$ ratios. CNO processing of the red giant envelope by meridional circulation begins on the upper subgiant branch or lower giant branch when the hydrogen shell reaches the hydrogen discontinuity produced by the convective envelope at the time of deepest penetration on the subgiant branch. The main-sequence angular velocity ω_{MS} needed for substantial CNO processing of the envelope has been computed by assuming that a star retains its interior angular momentum into the red giant phase. If the specific angular momentum is constant within the convective envelope of a red giant star, ω_{MS} is $\sim 10^{-4}$ rad s^{-1}. Such an angular velocity is plausible if one attributes the observed slow rotation rates of the lower main-sequence stars to a spin-down of the outer convective layers. Prohibitively large values of ω_{MS} are required if the entire convective envelope rotates instead as a solid body. This difficulty can be readily overcome if the inner part of the convective envelope departs from solid-body rotation. Reasons for such a departure are discussed. The distributions of the CNO elements near the hydrogen shell have been computed for several red giant models. The results show that there is a region of significant extent above the hydrogen shell within which carbon has been converted to nitrogen by the CN cycle. Closer to the hydrogen shell there is a region within which oxygen has been converted to nitrogen by the ON cycle. The gradient in the mean molecular weight μ within the carbon-depleted region is insufficient to inhibit the circulation currents for all values of the heavy-element abundance Z. The circulation currents are only likely to penetrate into the oxygen-depleted region for small values of Z due to a large μ gradient which otherwise exists in this region. The larger CN variations in globular-cluster giants might be due to more extensive ON processing of the mixed material, particularly for the extreme CN-strong stars in ω Cen. The envelopes of Population I giants only undergo CN processing, result ing in smaller CN variations. The lack of an observed correlation between the carbon depletions and nitrogen enhancements along the red giant branch of M92 might be caused by varying amounts of ON processing of the mixed material due to a range in the initial main-sequence angular velocity. Meridional circulation would also reduce the envelope $^{12}C/^{13}C$ ratio. Mass loss does not significantly affect the present results.

Subject headings: stars: abundances — stars: interiors — stars: late-type — stars: rotation

I. INTRODUCTION

A variety of spectral anomalies involving the CNO elements exists among the red giant stars in globular clusters and in the field. Well-known examples of these anomalous giants include the CH, weak G band (WGB) and CN-strong stars as well as stars having low $^{12}C/^{13}C$ ratios (Faber 1977). The CH stars seem to be exceedingly rare in globular clusters, with all of the known examples belonging to ω Cen and M22. The more common WGB and CN-strong stars are found preferentially in the metal-poor and metal-rich globular clusters, respectively (McClure and Norris 1977). Since the effective temperatures and surface gravities of these stars often coincide with those of normal giants, their anomalies cannot be attributed to atmospheric effects (Zinn 1973). Substantial variations in the envelope abundances of carbon, nitrogen, and possibly oxygen among giants of the same globular cluster are thus indicated.

The CH and subgiant-CH stars show enhancements of the *s*-process elements in addition to their CNO anomalies (Keenan 1942; Wallerstein and Greenstein 1964; Bond 1974; Sneden and Bond 1976), suggesting that these stars are produced in a fundamentally different way from the WGB and CN-strong stars. One exception would be those CN-strong stars which might actually be hot CH stars (Dickens and Bell 1976). The present paper will be concerned

only with stars whose anomalies are confined to the CNO elements, and therefore the CH stars will not be discussed.

Cannon (1912) first noticed that the G band of the CH molecule is unusually weak in some field giants. More recent investigations have examined the properties of these stars (Bidelman 1951; Greenstein and Keenan 1958; Dean, Lee, and O'Brien 1977) and have considerably increased the number of known examples (Bidelman and MacConnell 1973). The field WGB stars HR 6766 and HD 91805, analyzed by Sneden *et al.* (1978) and Cottrell and Norris (1978), respectively, possess substantial carbon deficiencies, nitrogen enhancements, and approximately normal oxygen abundances. The weakness of the bands of carbon-containing molecules other than CH implies a genuine carbon deficiency and not a peculiar shift in the molecular equilibrium (Hartoog, Persson, and Aaronson 1977; Sneden *et al.* 1978). According to Cottrell and Norris (1978) the field WGB stars are probably in the core-helium burning phase although some of them may still be on the first ascent of the red giant branch (RGB).

The discovery that WGB stars also exist in globular clusters was made by Zinn (1973) during his work on the asymptotic giant branch (AGB) stars of M92. Subsequent studies have both confirmed Zinn's findings for M92 (Butler, Carbon, and Kraft 1975; Carbon *et al.* 1979; Bell, Dickens, and Gustafsson 1979) and extended them to other globular clusters (Mallia 1975, 1977; Dickens and Bell 1976; Norris and Bessell 1977; Norris and Zinn 1977; Zinn 1977; Bell and Butler 1979). These studies agree on the systematics of the WGB effect, and from them the following conclusions can be drawn:

1. The WGB effect is found on both the RGB and the AGB but is more pronounced on the AGB, where the majority of stars possess weak G bands. A range in G band strengths is actually observed rather than a dichotomy between the weak and strong categories.
2. In M92 the WGB stars on both branches show carbon abundances depleted by as much as a factor of 10 relative to Fe. Nitrogen enhancements by factors as large as 10 are also observed, but they do not seem to be correlated with the degree of carbon depletion.
3. There is no evidence that variations in the Ca and Fe abundances are associated with the WGB effect.
4. The onset of the WGB effect occurs on the upper subgiant branch (SGB) or lower giant branch. The carbon anomalies become more prominent with increasing luminosity, indicating that the mechanism causing these anomalies operates during the first ascent of the RGB.

Norris and Zinn (1977) and Zinn (1977) have noticed an absence of WGB stars within ~ 0.8 mag of the tip of the RGB in a number of globular clusters. This fact, together with the pronounced WGB effect of the AGB stars, was initially interpreted as evidence for an additional mechanism that operated at some point during the evolution between the tip of the RGB and the AGB. However, the recent results of Bell, Dickens, and Gustafsson (1978, 1979) have demonstrated that the lack of WGB stars near the tip of the RGB is due to their lower effective temperatures and that the carbon abundances of these stars have actually been strongly depleted. The degree of carbon depletion and nitrogen enhancement obtained for stars near the tip of the RGB in M92 by Carbon *et al.* (1979) agrees with that shown by the AGB stars. Consequently there is no compelling observational evidence for an additional mechanism operating beyond the RGB phase.

Among Population I stars the strength of the CN bands does not vary greatly and is known to be well correlated with [Fe/H] (Harmer and Pagel 1973; Janes 1975; Deming, Olson, and Yoss 1977). Just the opposite is true in the globular clusters, where the large observed CN variations (Bell, Dickens, and Gustafsson 1975, 1978; Bessell and Norris 1976; Hesser, Hartwick, and McClure 1976, 1977) show no obvious correlation with [Fe/H]. McClure and Norris (1977) have argued quite plausibly that the CN-strong and WGB effects are different manifestations of the same phenomenon. Carbon and nitrogen variations in globular clusters would be most readily detected through their effects on the CH bands in metal-poor stars and the CN bands in metal-rich stars.

Values of the $^{12}C/^{13}C$ ratio have been determined for a large number of field red giant stars (Dearborn, Lambert, and Tomkin 1975; Tomkin, Luck, and Lambert 1976). Standard stellar evolution calculations predict a reduction in the $^{12}C/^{13}C$ ratio to a value between 20 and 30 during the SGB phase when the convective envelope penetrates into the region that underwent CN processing during the main-sequence phase (Iben 1964, 1967). Such a reduction is observed in approximately 50 percent of the field giants. However, the remaining field giants have $^{12}C/^{13}C$ ratios below 20 and hence cannot be explained by this mechanism (Scalo and Miller 1978). The $^{12}C/^{13}C$ ratio tends to decrease with increasing luminosity, suggesting that low $^{12}C/^{13}C$ ratios might be produced during the RGB phase (Dearborn, Eggleton, and Schramm 1976; Tomkin, Luck, and Lambert 1976).

The most straightforward interpretation of the above observations is that the envelopes of the anomalous giants have undergone partial nuclear processing by the CNO cycle. Such processing would convert carbon (and perhaps also oxygen) into nitrogen and would lower the $^{12}C/^{13}C$ ratio. This attractive explanation is not, however, supported by stellar model computations which consistently show that the temperature at the base of the convective envelope in red giant stars of a few solar masses or less remains too low for the operation of either the CN or ON cycle (Sweigart and Gross 1978). Only at luminosities greater than $\sim 10^4 L_\odot$ might the base temperature become sufficiently high (Scalo, Despain, and Ulrich 1975), but such luminosities far exceed those of the giants being considered here. The partial CNO processing of the envelope thus requires mixing into the hotter region just above the hydrogen shell. However, a radiative zone, spanning roughly five orders of magnitude in pressure, separates this hotter region from the convective envelope (Sweigart and Gross 1978), and consequently no mixing across this zone occurs in red giant models constructed with the standard assumptions. The principal problem

therefore is to identify the mechanism responsible for mixing CNO-processed material from the vicinity of the hydrogen shell into the envelope.

The main objective of the present paper is to examine the possibility that meridional circulation driven by internal rotation might produce the required mixing. We will attempt to demonstrate that reasonable rates of rotation are sufficient to cause substantial CNO processing of the envelope during the available red giant lifetime and that meridional circulation might thus provide a plausible explanation for many of the observed CNO anomalies. We do not exclude the possibility that primordial variations in the composition may also be involved to some extent, particularly in the peculiar globular cluster ω Cen, where there is observational evidence for primordial variations in the metal abundance (Freeman and Rodgers 1975; Norris and Bessell 1977; Butler, Dickens, and Epps 1978). Nevertheless, the present paper will only investigate the extent to which mixing by itself can account for the observed anomalies.

Meridional circulation during the main-sequence phase has been proposed by Paczyński (1973) to account for the low C/N ratios in some early type stars and, more recently, has been suggested by Cottrell and Norris (1978) as the cause of the WGB effect in Population I stars. In contrast, the emphasis in the present paper is on meridional circulation that occurs during the red giant phase. Some comments on whether meridional circulation can lead to significant mixing during the main-sequence phase of low-mass stars will, however, be included in § IV*d*.

Several other explanations have been advanced to account for the observed CNO anomalies. In general, these explanations either are not fully consistent with the observational data or encounter significant theoretical difficulties. One type of such explanations involves thermal instabilities—i.e., hydrogen-shell flashes, the helium-core flash, and helium-shell flashes. Several objections can be raised against each of these possibilities. The detailed stability analysis of red giant models by Gabriel and Noels (1974) revealed no instability of the hydrogen shell during the SGB phase when instability would be most likely to occur (Bolton and Eggleton 1973). As far as the authors are aware, no hydrogen-shell flash has ever been computed for a red giant star. If hydrogen-shell flashes were a normal characteristic of red giant evolution, it would be difficult to understand the variations in the CNO anomalies from star to star. Hydrogen-shell flashes are also unlikely to produce low $^{12}C/^{13}C$ ratios for the following reason (Dearborn, Bolton, and Eggleton 1975; Dearborn, Eggleton, and Schramm 1976). During a flash one would expect a temporary convective zone to develop within the hydrogen shell. If this convective zone reached into the ^{13}C peak above the hydrogen shell (see § II), the ^{13}C would be mixed inward to higher temperatures and hence rapidly destroyed. Consequently any material mixed into the envelope after a flash would probably be fully processed to CNO equilibrium and would thus contain little ^{13}C. Most of the envelope would then have to be processed in order to achieve a significant reduction in the $^{12}C/^{13}C$ ratio.

Following a helium-core flash, the base of the convective envelope might extend briefly into the hydrogen shell. Because the hydrogen shell then contains very little mass ($\sim 5 \times 10^{-4}\ M_\odot$), the amount of CNO-processed material mixed into the envelope would be insufficient to change significantly the envelope CNO abundances. A deeper penetration of the convective envelope through the hydrogen shell and into the core, as found by Thomas (1967) and Paczyński and Tremaine (1977), would add carbon to the envelope, just the opposite of what is required for the WGB effect. To be consistent with the observations, one would have to speculate that the carbon is converted to nitrogen during the mixing process. However, the temperature at the base of the convective envelope remains too low during the inward penetration for such CN processing to take place (Mengel and Sweigart 1979). Furthermore, CNO anomalies are observed in stars apparently on their first ascent of the RGB (Norris 1978; Hesser 1978).

The helium-shell flashes can likewise be ruled out as a possible explanation, since they do not occur until a star reaches a luminosity of about $10^3\ L_\odot$ (Sweigart 1973; Gingold 1974). Most of the anomalous giants have lower luminosities, and some clearly belong to the RGB. Only for very luminous giants might the helium-shell flashes modify the CNO abundances (Gingold 1974).

In the following section we examine the distribution of the CNO elements in the neighborhood of the hydrogen shell for several representative red giant models. The dependence of the amount of meridional mixing on the initial main-sequence angular velocity is determined in § III, where we compute the main-sequence angular velocities which can lead to substantial CNO processing of the envelope. Section IV compares the present results with the observational data. We consider the following questions. Are the main-sequence angular velocities required by the present theory of meridional mixing reasonable? Under what circumstances does the ON cycle participate in the CNO processing? Could such ON participation be related to the lack of correlation between the carbon depletions and nitrogen enhancements in M92 and to the larger CN variations in the globular cluster stars? At what luminosity does the meridional mixing begin? We also discuss the uncertainties involved in the present calculations. Finally § V summarizes our main conclusions.

II. CNO PROFILES NEAR THE HYDROGEN SHELL

When a star evolves off the main sequence, the convective envelope moves inward in mass until deepest penetration occurs on the SGB. At that time the convective envelope extends into the region where hydrogen was partially depleted during the main-sequence phase. A discontinuity in the hydrogen abundance is then formed at the point of deepest penetration. With the later approach of the hydrogen shell, the convective envelope retreats outward, leaving behind a chemically homogeneous radiative zone.

In order for the circulation currents to affect the envelope CNO abundances, two conditions must be fulfilled. First, the radiative zone separating the convective envelope from the hydrogen shell must not have a significant gradient in the mean molecular weight μ, since μ gradients tend to inhibit meridional circulation (Mestel 1953, 1957); second, the temperature at the base of the region reached by the circulation currents must be sufficiently high for at least CN processing. Neither of these conditions is fulfilled before the hydrogen shell reaches the hydrogen discontinuity. The μ barrier formed by this discontinuity and by the hydrogen gradient inside this discontinuity effectively prevents the circulation currents from reaching the hydrogen shell. Although the homogeneous zone can support circulation currents, the temperature at its base remains quite low as long as the hydrogen discontinuity exists. We conclude that CNO processing of the envelope by meridional mixing cannot begin until the hydrogen shell has burned through the hydrogen discontinuity. This occurs along the upper SGB or lower RGB, depending on the composition and mass.

Of particular interest are the distributions of the CNO elements in the vicinity of the hydrogen shell after the hydrogen discontinuity has burned away. These distributions determine how deeply the circulation currents must penetrate in order to dredge up CNO-processed material. If a deep penetration into the hydrogen shell is necessary, the circulation currents would be choked off by the μ gradient of the shell, and meridional circulation could not then provide the required mixing.

Although the temperatures of the layers just above the hydrogen shell are too low for the full CNO cycle to operate in equilibrium, the processing of carbon into nitrogen through the $^{12}C(p, \gamma)^{13}N(\beta^+\nu)^{13}C(p, \gamma)^{14}N$ reactions of the CN cycle might still proceed at a significant rate. At the higher temperatures closer to the hydrogen shell the slower $^{16}O(p, \gamma)^{17}F(\beta^+\nu)^{17}O(p, \alpha)^{14}N$ reactions of the ON cycle might also take place, thus converting oxygen into nitrogen. Upon going inward toward the hydrogen shell, one might therefore expect to encounter first a shell in which carbon is burned to nitrogen, then a region depleted of carbon and finally a shell in which oxygen is burned to nitrogen. Since only 2 protons are needed to transform one ^{12}C nucleus to ^{14}N, the hydrogen abundance and hence μ will remain essentially constant across the carbon shell even for Population I carbon abundances (Paczyński 1973). However, a larger change in μ will exist across the oxygen shell due to the greater amount of hydrogen burning which occurs during the approach to ON equilibrium.

The properties of the carbon and oxygen shells have been investigated by the following procedure. For several red giant models chosen from the evolutionary sequences of Sweigart and Gross (1978), we obtained the run of temperature and density in the vicinity of the hydrogen shell. The differential equations for the approach to CNO equilibrium (Clayton 1968) were then integrated by assuming that the carbon and oxygen shells had "stationary profiles," i.e., that the distributions of carbon and oxygen relative to the hydrogen shell were not changing with time. This is an excellent approximation, as shown by the fact that the hydrogen-shell profile changes very slowly along the RGB. The assumption of stationary profiles permits one to replace the time derivatives of the CNO abundances by derivatives with respect to the mass coordinate M_r according to the equation

$$\frac{d}{dt} = \frac{L_H}{EX_{env}} \frac{d}{dM_r}, \tag{1}$$

where L_H, E, and X_{env} are, respectively, the total hydrogen-burning luminosity, the energy released per gram of hydrogen burned, and the mass fraction of hydrogen in the envelope. A similar substitution for the time derivative has been used in other contexts by Eggleton (1967, 1968) and Paczyński (1970). The rates for the various CNO reactions were taken from Fowler, Caughlan, and Zimmerman (1975). Surface values for the relative abundances of the CNO elements were those given by Cox and Stewart (1970). Since the reaction rates are proportional to the abundances, the absolute abundances are not important for determining the locations of the shells. We have also assumed that the surface $^{12}C/^{13}C$ ratio is 30, as predicted by standard evolutionary sequences, but again the precise value is not important.

Figure 1 shows the distributions of the CNO elements near the hydrogen shell of a red giant model chosen to represent a typical metal-poor globular cluster giant shortly after the onset of the meridional mixing. The parameters of the model in Figure 1 are $(M, Y, Z) = (0.90, 0.20, 0.0001)$ and $\log L = 2.31$. Here the helium abundance Y refers to the main-sequence phase and thus does not include the slight helium enrichment which occurs during the inward excursion of the convective envelope on the SGB (see Table 1 of Sweigart and Gross 1978). M and Z are the total mass and heavy-element abundance, respectively. Figure 1 demonstrates that a substantial carbon-depleted region exists above the hydrogen shell. The negligible μ gradient across the carbon shell would not be able to prevent the circulation currents from reaching into this region. As expected, the oxygen shell is located much closer to the hydrogen shell, although it is still well separated from the hydrogen shell in the present case. At the midpoint of the oxygen shell the hydrogen abundance X has been depleted by only 0.0004 from its envelope value. Since the μ gradient at the oxygen shell is rather small, it is likely that ON-processed material would also be accessible to the circulation currents, especially for the faster rotators.

Similar computations have been carried out for two other metal-poor red giant models with $(M, Y, Z) = (0.70, 0.30, 0.0001)$ and $\log L = 2.66$ and 3.17. The CNO distributions in the $\log L = 2.66$ case agree closely with those shown in Figure 1, and in particular the separations between the various shells are roughly the same. The results for these two models indicate that the extent of the carbon-depleted region decreases with increasing

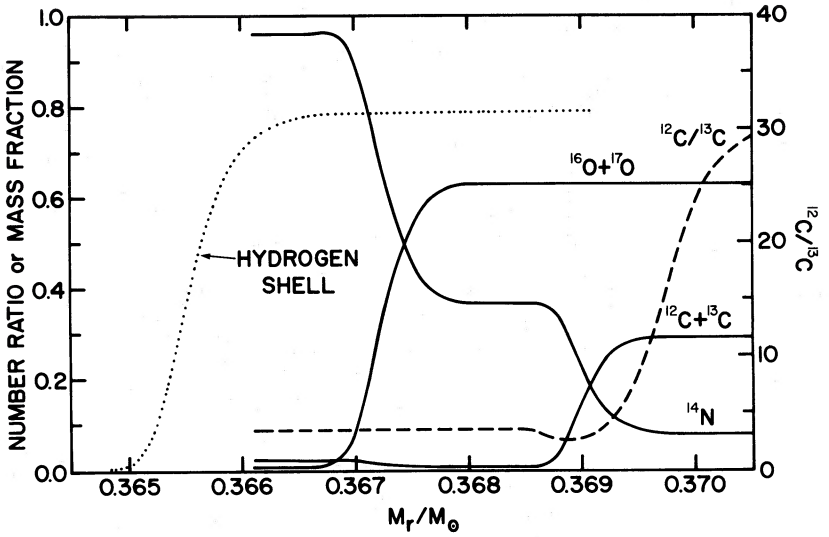

FIG. 1.—Distributions of the CNO elements in the vicinity of the hydrogen shell of a red giant model with the parameters $(M, Y, Z) = (0.90, 0.20, 0.0001)$ and $\log L = 2.31$. The three solid curves, which use the left vertical scale, give the abundance by number of $^{12}C + {}^{13}C$, ^{14}N and $^{16}O + {}^{17}O$ expressed as fractions of the total number of CNO nuclei. The dotted curve represents the hydrogen abundance X by mass (*left vertical scale*), while the dashed curve gives the number ratio $^{12}C/^{13}C$ (*right vertical scale*).

luminosity. For example, the difference in M_r between the midpoints of the hydrogen and carbon shells decreases from 0.0028 to 0.0016 $M_\odot$ in going from $\log L = 2.66$ to 3.17.

The CNO distributions near the hydrogen shell of a metal-rich globular cluster star with $(M, Y, Z) = (0.90, 0.20, 0.004)$ and $\log L = 2.22$ are illustrated in Figure 2. The main effect of increasing Z is to shift the carbon and oxygen shells inward toward the hydrogen shell. This effect can be readily understood. Consider two red giant models which differ only in their values of Z. In order for L_H to be the same in both models, the temperatures near the hydrogen shell of the higher Z model must be somewhat lower to compensate for the higher CNO abundance. As a result, the temperatures needed for CN or ON processing are only attained closer to the hydrogen shell.

In Figure 2 the carbon and hydrogen shells are again well separated, and consequently the μ gradient across the carbon shell remains quite negligible. However, the oxygen shell is now situated at the upper edge of the hydrogen shell, where the μ gradient is becoming appreciable. The amount of hydrogen depletion at the midpoint of the oxygen shell has increased to 0.021. It is no longer clear whether the circulation currents can overcome the μ

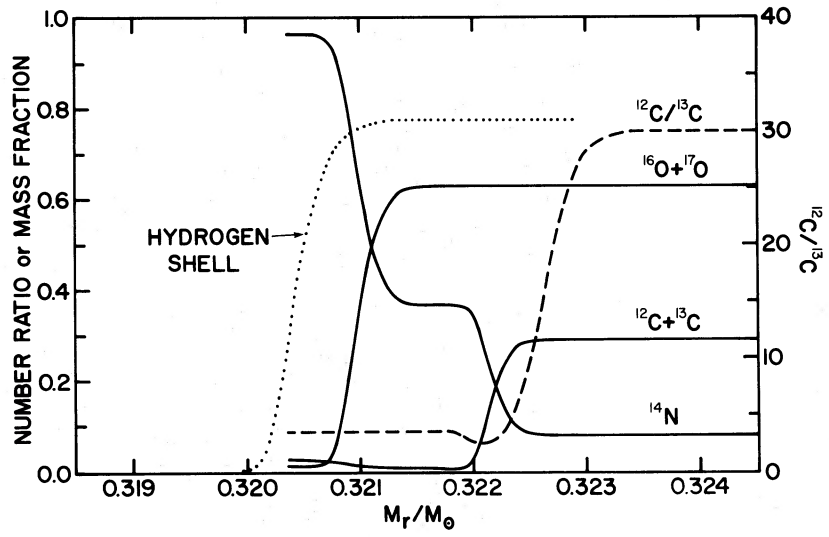

FIG. 2.—Distributions of the CNO elements in the vicinity of the hydrogen shell of a red giant model with the parameters $(M, Y, Z) = (0.90, 0.20, 0.004)$ and $\log L = 2.22$. The meanings of the various curves are the same as explained in the legend for Fig. 1.

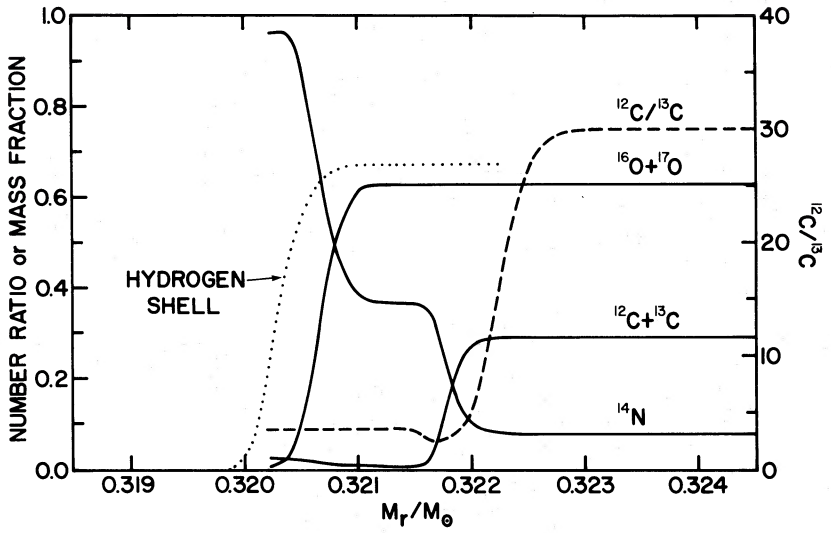

FIG. 3.—Distributions of the CNO elements in the vicinity of the hydrogen shell of a red giant model with the parameters $(M, Y, Z) = (1.40, 0.30, 0.01)$ and $\log L = 2.37$. The meanings of the various curves are the same as explained in the legend for Fig. 1.

gradient around the oxygen shell, since the theoretical estimates for the size of the μ gradient needed to stop the meridional circulation are very uncertain (see § IV*d*).

To represent a Population I giant, we have chosen a red giant model with the parameters $(M, Y, Z) = (1.40, 0.30, 0.01)$ and $\log L = 2.37$. This choice for the mass seems appropriate in view of the estimates for the masses of Population I WGB stars (Sneden *et al.* 1978; Cottrell and Norris 1978). Moreover, Scalo and Miller (1978) have argued that the mechanism producing the low $^{12}C/^{13}C$ ratios must operate in stars with masses of 1.5 $M_\odot$ or less. The CNO distributions for this model are given in Figure 3, where a further inward shift of the carbon and oxygen shells is again evident. The circulation currents must now go significantly into the hydrogen shell in order to dredge up ON-processed material. In the present case the μ barrier of the hydrogen shell would probably shield the ON-processed region from the circulation currents, and hence ON processing of the envelope by meridional mixing would not be expected.

The above computations have neglected the effects which the meridional mixing has on the CNO distributions. Such mixing might distort the stationary profiles shown in Figures 1–3 and might alter the positions of the carbon and oxygen shells by an amount depending on the rotation rate. Nevertheless, the following conclusions should be secure:

1. A carbon-depleted region of significant extent exists above the hydrogen shell of a red giant star. Closer to the hydrogen shell there is a region in which the ON cycle has converted oxygen to nitrogen. The mass extent of these carbon- and oxygen-depleted regions decreases as Z increases.
2. For all values of Z the carbon shell is well separated from the hydrogen shell so that the μ gradient cannot prevent the circulation currents from reaching into the carbon-depleted region.
3. For low values of Z the oxygen shell is also sufficiently well separated from the hydrogen shell that ON-processed material can probably be mixed into the envelope, at least for the more rapidly rotating stars. However, an increase in Z reduces the likelihood of ON processing of the envelope because of the μ gradient which develops within the oxygen-depleted region. For Population I compositions this μ gradient is sufficiently large that ON processing becomes unlikely. The precise value of Z at which ON processing is no longer important is not certain. There is a general trend for the ON processing to be restricted to stars with progressively faster rotation rates as Z increases.

In the next section we investigate whether the meridional mixing can proceed rapidly enough to process the envelope material during the available red giant lifetime.

III. CNO MIXING BY MERIDIONAL CIRCULATION

a) Preliminary Discussion

Because rotation leads to deviations from spherical symmetry, a rotating star cannot simultaneously fulfill the conditions of hydrostatic and thermal equilibrium everywhere on an equipotential surface (von Zeipel 1924; Baker and Kippenhahn 1959). This difficulty forces a star to set up circulation currents which compensate at each point for a nonzero divergence of the radiation flux (Eddington 1925, 1929; Vogt 1925). The velocity v_{EV} of these Eddington-Vogt circulation currents was first estimated by Sweet (1950).

In order to evaluate the rate of meridional mixing, we will make several assumptions. These assumptions are (1) that on the main sequence a star rotates as a solid body with the angular velocity ω_{MS}, (2) that a star's interior retains its angular momentum into the red giant phase, and (3) that each mass shell conserves its angular momentum after leaving the convective envelope. A discussion of these assumptions is postponed until § IV.

Kippenhahn (1974) has obtained an approximate expression for the circulation velocity, namely,

$$v_{EV} \approx \frac{\nabla_{ad}}{(\nabla_{ad} - \nabla)} \frac{L_r \chi_r}{M_r} \frac{3}{4\pi r G \rho}, \tag{2}$$

where χ_r, the local ratio of the centrifugal to gravitational forces, is given by

$$\chi_r = \frac{r^3 \omega_r^2}{G M_r}, \tag{3}$$

and where ω_r is the angular velocity at the mass point M_r. The other symbols have their usual meanings. Equation (2) assumes slow rotation and nondegenerate matter. As will be seen later, the rotation rates required for substantial mixing are very mild ($\chi_r \ll 1$) and thus should not appreciably perturb the interior structure. Consequently we can take the quantities other than ω_r from standard nonrotating red giant models without significantly affecting our results. If we assume that matter is flowing inward over one-half of an equipotential surface and outward over the remaining one-half, then the rate dM_{CNO}/dt at which CNO-processed material is being injected into the envelope is given by

$$\frac{dM_{CNO}}{dt} = 2\pi r^2 \rho v_{EV}. \tag{4}$$

To specify quantitatively when substantial CNO processing of the envelope has occurred, we adopt the following criterion: the amount of CNO-processed material mixed into the envelope between the onset of the meridional mixing and the helium-core flash must equal the envelope mass at the time when the meridional mixing begins. Let t denote the time elapsed since the zero-age main-sequence phase, and M_{sh} the amount of mass interior to the center of the hydrogen shell. The envelope mass M_{env} is simply $M - M_{sh}$. Our criterion then becomes

$$\int_{t^*}^{t_f} \frac{dM_{CNO}}{dt}\, dt = M_{env}^*, \tag{5}$$

where the subscript f refers to the helium-core flash and the asterisk refers to the onset of the meridional mixing, i.e., the time when the hydrogen shell reaches the hydrogen discontinuity.

If dM_{CNO}/dt is evaluated at the top of the hydrogen shell, we can replace M_r by M_{sh}, since the hydrogen shell is very thin in mass. Combining equations (2) to (4) then yields

$$\frac{dM_{CNO}}{dt} = \frac{3}{2G^2} \frac{\nabla_{ad}}{(\nabla_{ad} - \nabla)} L_r \frac{r^4 \omega_r^2}{M_{sh}^2}. \tag{6}$$

In the radiative zone the outward flux L_r is essentially the same as the hydrogen luminosity L_H, which in turn is related to the rate at which hydrogen is being consumed by the expression

$$L_H = E X_{env} \frac{dM_{sh}}{dt}. \tag{7}$$

If equation (7) is substituted for L_r in equation (6), it is possible to replace the time derivative of M_{CNO} by a derivative with respect to M_{sh}. Equation (6) then becomes

$$\frac{dM_{CNO}}{dM_{sh}} = \frac{3 E X_{env}}{2G^2} \frac{\nabla_{ad}}{(\nabla_{ad} - \nabla)} \frac{r^4 \omega_r^2}{M_{sh}^2}. \tag{8}$$

We now define a function $F(M_{sh})$ by

$$F(M_{sh}) = \frac{3 E X_{env}}{2G^2} \left\langle \frac{\nabla_{ad}}{(\nabla_{ad} - \nabla)} \right\rangle \int_{M_{sh}^*}^{M_{sh}} \frac{r^4 \omega_r^2}{M_{sh}^2}\, dM_{sh}, \tag{9}$$

where M_{sh}^* denotes the value of M_{sh} at the onset of meridional mixing. The function $F(M_{sh})$ represents the amount of CNO-processed material added to the envelope by the time the hydrogen shell reaches M_{sh}. The quantity $\nabla_{ad}/(\nabla_{ad} - \nabla)$ has been removed from the integrand, since it is roughly constant during the evolution. A mean

value of 3 has been adopted for this quantity in all computations. We note that $F(M_{sh})$ is proportional to ω_r^2 and hence to ω_{MS}^2. In terms of $F(M_{sh})$, criterion (5) can be written more succinctly as

$$F(M_c) = M_{env}^*, \tag{10}$$

where the core mass M_c is simply the value of M_{sh} at the helium-core flash.

The determination of the amount of CNO processing has now been reduced to the problem of evaluating the function $F(M_{sh})$. To accomplish this, we must know how the angular momentum is distributed within the deep convective envelope of a red giant star. The angular velocity ω_r of a layer near the hydrogen shell depends on how much angular momentum is left behind as the convective envelope retreats outward. Consequently the integral in equation (9) is basically determined by the amount of angular momentum within the inner part of the convective envelope. Unfortunately the distribution of angular momentum within the convective envelope is not understood theoretically. There are two limiting cases which need to be considered, namely, the case in which the specific angular momentum is the same at all points within the convective envelope and the case in which the convective envelope rotates as a solid body (Tayler 1973; Endal 1976). In the following two subsections, we will compute the function $F(M_{sh})$ for each of these cases.

Before continuing, we define a number of quantities which will prove useful in the subsequent discussion. The total angular momentum and moment of inertia of the convective envelope will be denoted by J_{CE} and I_{CE}, respectively, while M_{CE} will stand for the value of M_r at the base of the convective envelope. We let J_{DP} and M_{DP} represent the values of J_{CE} and M_{CE}, respectively, at the time of deepest penetration of the convective envelope on the SGB. It follows that $M_{DP} = M_{sh}^*$. The quantities J_{MS} and I_{MS} will give the total angular momentum and moment of inertia, respectively, of the layers with $M_r \geq M_{DP}$ at the zero-age main-sequence phase. Our previous assumption that the interior angular momentum is retained into the red giant phase means that $J_{DP} = J_{MS}$.

b) Case 1: Constant Specific Angular Momentum within the Convective Envelope

When a mass shell detaches from the base of the convective envelope, the angular momentum J_{CE} of the convective envelope decreases. In the present case, however, the specific angular momentum of the shell is the same as the specific angular momentum j_{CE} of the matter within the convective envelope, and consequently there is no change in the value of j_{CE}. At any point along the RGB, j_{CE} will thus be equal to its value at the time of deepest penetration of the convective envelope on the SGB. We therefore have

$$j_{CE} = \frac{J_{DP}}{M - M_{DP}}. \tag{11}$$

Since $J_{DP} = J_{MS}$, equation (11) implies that $j_{CE} = \bar{j}_{MS}$ with $\bar{j}_{MS}$ being the average specific angular momentum of the layers with $M_r \geq M_{DP}$ at the zero-age main-sequence phase. Because the angular momentum of a mass shell is assumed to be conserved after the shell leaves the convective envelope, it follows that the specific angular momentum $j(=r^2\omega_r)$ at the top of the hydrogen shell equals j_{CE} and thus $\bar{j}_{MS}$. The factor $r^4\omega_r^2$ in equation (9) is therefore constant during the evolution and can be removed from the integral. Since the integration is then trivial, we readily obtain the desired expression for $F(M_{sh})$:

$$F(M_{sh}) = \frac{3EX_{env}}{2G^2}\left\langle \frac{\nabla_{ad}}{(\nabla_{ad} - \nabla)} \right\rangle \bar{j}_{MS}^2 \left[\frac{1}{M_{sh}^*} - \frac{1}{M_{sh}}\right]. \tag{12}$$

By imposing the criterion that $F(M_c) = M_{env}^*$, one can determine the value of $\bar{j}_{MS}$ needed for substantial CNO processing of the envelope. The main-sequence angular velocity ω_{MS} then follows from

$$\omega_{MS} = \frac{\bar{j}_{MS}(M - M_{DP})}{I_{MS}}. \tag{13}$$

Values of ω_{MS} obtained in this manner are listed in Table 1 for four evolutionary sequences covering the range in Z from 0.0001 to 0.01. These particular sequences were selected to represent metal-poor and metal-rich globular cluster stars as well as Population I stars. In the present case of constant j_{CE} the required values of ω_{MS} are all $\sim 6 \times 10^{-5}$ rad s^{-1}, a value which is rather modest compared with the interior angular velocities one might expect in main-sequence stars (see § IV*a*). These results do not significantly depend on the value of the ratio of mixing length l to pressure scale height H_p used in constructing the models. Changing l/H_p in a red giant model does change r and ω_r in the convective envelope, but not j_{CE}. Furthermore, changes in l/H_p only slightly affect M_{sh}^* and I_{MS} (Sweigart 1979).

The physical conditions prevailing at the midpoints of the hydrogen, oxygen, and carbon shells, at the base of the convective envelope and at the surface are shown in Table 2 for a representative red giant model from each of the sequences of Table 1. The models in columns (1), (3), and (4) are the same as those used in computing the stationary profiles in Figures 1, 2, and 3, respectively. A subscript s refers to the surface. The values of the various rotation quantities are based on the values of ω_{MS} given in Table 1. It is apparent from the data of Table 2 that

TABLE 1

MAIN-SEQUENCE ANGULAR VELOCITIES FOR MERIDIONAL MIXING

Parameter	Evolutionary Sequence			
M	0.90	0.70	0.90	1.40
Y	0.20	0.30	0.20	0.30
Z	0.0001	0.0001	0.004	0.01
X_{env}	0.7870	0.6948	0.7750	0.6747
M^*_{env}	0.5368	0.3420	0.6229	1.1090
M^*_{sh}	0.3632	0.3580	0.2771	0.2910
M_c	0.5078	0.4886	0.4896	0.4632
log I_{MS}	53.598	53.342	53.628	53.954
$t_f - t^*$ (10^6 yrs)	20.730	15.705	59.473	26.443
ω_{MS}†	6.4×10^{-5}	6.4×10^{-5}	5.3×10^{-5}	7.1×10^{-5}
log j_{MS}†	16.377	16.317	16.262	16.462
log J_{MS}†	49.405	49.149	49.355	49.805
ω_{MS}§	2.0×10^{-3}	1.3×10^{-3}	1.5×10^{-3}	5.0×10^{-3}
log j_{MS}§	17.868	17.610	17.707	18.314
log J_{MS}§	50.896	50.442	50.800	51.657

† Refers to the case of constant specific angular momentum within the red-giant convective envelope.

§ Refers to the case of solid-body rotation of the red-giant convective envelope.

the angular velocities required by the present theory of meridional mixing only slightly perturb the interior structure. In the vicinity of the hydrogen, oxygen, and carbon shells χ_r is $\sim 10^{-2}$ or less, while at the base of the convective envelope and at the surface χ_r decreases to $\sim 10^{-4}$ and $\sim 10^{-6}$, respectively. The surface rotation velocity v_s is only ~ 0.1 km s^{-1} and hence undetectable. Our use of nonrotating models in the present calculations is therefore justified. A discussion of how the amount of CNO processing varies along the RGB will be postponed to § IV*c*.

c) Case 2: Solid-Body Rotation of the Convective Envelope

The integrand in equation (9) involves the angular velocity ω_r near the top of the hydrogen shell. By assumption the specific angular momentum $r^2\omega_r$ of any mass shell within the radiative zone above the hydrogen shell is equal to the specific angular momentum $r_b^2\omega_{CE}$ which the mass shell had when it detached from the convective envelope. Here ω_{CE} is the angular velocity of the convective envelope, and r_b is the radius at its base. Since for solid-body rotation $\omega_{CE} = J_{CE}/I_{CE}$, it follows that $r^2\omega_r = r_b^2 J_{CE}/I_{CE}$. To compute ω_r therefore requires that we know r_b, J_{CE}, and I_{CE} at the moment of detachment. Both r_b and I_{CE} can be obtained from the red giant sequences of Sweigart and Gross (1978) so that the problem reduces to one of determining J_{CE}. As a mass shell dM_{CE} leaves the convective envelope, it carries away an amount of angular momentum $dJ_{CE} = -\frac{2}{3}r_b^2\omega_{CE}dM_{CE} = -\frac{2}{3}r_b^2 \times (J_{CE}/I_{CE})dM_{CE}$, where the geometrical factor of $\frac{2}{3}$ comes from averaging over all directions. Integration of this differential equation yields

$$J_{CE} = J_{DP} \exp\left[-\int_{M_{DP}}^{M_{CE}} \frac{2}{3}\frac{r_b^2}{I_{CE}}\, dM_{CE} \right] \tag{14}$$

for the angular momentum J_{CE} as a function of M_{CE}. This integral has been evaluated for a red giant sequence with $(M, Y, Z) = (0.70, 0.30, 0.0001)$. We find that J_{CE} differs from J_{DP} by less than 1% at all points along the RGB, and hence to an excellent approximation J_{CE} may be regarded as a constant. This result is physically reasonable, since for solid-body rotation there is very little angular momentum near the base of the convective envelope due to the relatively small value of r_b. Using the fact that $J_{CE} \approx J_{DP} = J_{MS} = I_{MS}\omega_{MS}$, we can rewrite equation (9) in the form

$$F(M_{sh}) = \frac{3EX_{env}}{2G^2}\left\langle \frac{\nabla_{ad}}{(\nabla_{ad} - \nabla)} \right\rangle I_{MS}^2\omega_{MS}^2 \int_{M_{sh}^*}^{M_{sh}} \frac{r_b^4}{I_{CE}^2}\frac{dM_{sh}}{M_{sh}^2}, \tag{15}$$

where the integrand is to be evaluated at the time when M_r at the base of the convective envelope equals M_{sh}. For each red giant sequence in Table 1, I_{CE} was computed for a model shortly after the onset of meridional mixing. To obtain I_{CE} at other points along the RGB, we assumed that $I_{CE} \propto (M - M_{CE})R^2$, where R is the surface radius. This approximation affects the value of the integral in equation (15) by roughly 15%.

From the criterion that $F(M_c) = M_{env}^*$, we can now derive the value of ω_{MS} needed for substantial CNO processing in each of the sequences of Table 1. The values of ω_{MS} thus computed range from 10^{-3} to 5×10^{-3} rad s^{-1} (see Table 1) and thus are considerably greater than the values previously obtained for the constant j_{CE} case.

TABLE 2

EFFECTS OF ROTATION ON SELECTED RED GIANT MODELS

Parameter	Red-Giant Model			
M	0.90	0.70	0.90	1.40
Y	0.20	0.30	0.20	0.30
Z	0.0001	0.0001	0.004	0.01
Middle of hydrogen shell:				
M_r	0.3655	0.3964	0.3204	0.3203
log r	9.266	9.276	9.296	9.326
log ρ	2.197	2.079	1.949	1.834
log T	7.648	7.692	7.560	7.556
X	0.3935	0.3474	0.3875	0.3374
ω_r†	7.0×10^{-3}	5.8×10^{-3}	4.7×10^{-3}	6.4×10^{-3}
χ_r†	6.3×10^{-3}	4.3×10^{-3}	4.0×10^{-3}	9.3×10^{-3}
ω_r§	1.5×10^{-2}	5.8×10^{-3}	2.8×10^{-3}	7.9×10^{-3}
χ_r§	3.0×10^{-2}	4.3×10^{-3}	1.4×10^{-3}	1.4×10^{-2}
Middle of oxygen shell:				
M_r	0.3672	0.3978	0.3210	0.3207
log r	9.435	9.450	9.369	9.377
log ρ	1.500	1.372	1.549	1.523
log T	7.493	7.532	7.496	7.513
X	0.7866	0.6945	0.7539	0.6310
ω_r†	3.2×10^{-3}	2.6×10^{-3}	3.3×10^{-3}	5.1×10^{-3}
χ_r†	4.3×10^{-3}	2.9×10^{-3}	3.4×10^{-3}	8.3×10^{-3}
v_{EV} (cm s^{-1})†	5.5×10^{-4}	1.1×10^{-3}	3.8×10^{-4}	1.2×10^{-3}
ω_r§	6.2×10^{-3}	2.5×10^{-3}	1.9×10^{-3}	6.2×10^{-3}
χ_r§	1.6×10^{-2}	2.7×10^{-3}	1.1×10^{-3}	1.2×10^{-2}
v_{EV} (cm s^{-1})§	2.1×10^{-3}	1.0×10^{-3}	1.3×10^{-4}	1.8×10^{-3}
Middle of carbon shell:				
M_r	0.3690	0.3992	0.3222	0.3218
log r	9.625	9.633	9.554	9.558
log ρ	0.940	0.821	0.978	0.945
log T	7.311	7.352	7.314	7.335
X	0.7870	0.6948	0.7750	0.6747
ω_r†	1.3×10^{-3}	1.1×10^{-3}	1.4×10^{-3}	2.2×10^{-3}
χ_r†	2.7×10^{-3}	1.9×10^{-3}	2.2×10^{-3}	5.4×10^{-3}
v_{EV} (cm s^{-1})†	8.0×10^{-4}	1.6×10^{-3}	6.2×10^{-4}	2.4×10^{-3}
ω_r§	2.4×10^{-3}	1.1×10^{-3}	8.0×10^{-4}	2.6×10^{-3}
χ_r§	8.5×10^{-3}	1.7×10^{-3}	6.9×10^{-4}	7.4×10^{-3}
v_{EV} (cm s^{-1})§	2.5×10^{-3}	1.4×10^{-3}	2.0×10^{-4}	3.2×10^{-3}
Base of convective envelope:				
M_r	0.3976	0.4191	0.3355	0.3350
log r	11.096	11.218	10.926	10.966
log ρ	-2.630	-3.243	-2.484	-2.582
log T	6.110	5.996	6.209	6.228
X	0.7870	0.6948	0.7750	0.6747
ω_r†	1.5×10^{-6}	7.6×10^{-7}	2.6×10^{-6}	3.4×10^{-6}
χ_r†	8.6×10^{-5}	4.7×10^{-5}	8.9×10^{-5}	2.0×10^{-4}
ω_r§	1.9×10^{-6}	5.1×10^{-7}	1.1×10^{-6}	2.6×10^{-6}
χ_r§	1.3×10^{-4}	2.1×10^{-5}	1.6×10^{-5}	1.2×10^{-4}
Total star:				
log L_H	2.310	2.655	2.216	2.363
log L	2.313	2.659	2.218	2.365
log T_{eff}	3.645	3.629	3.594	3.590
log R	12.236	12.440	12.290	12.372
log g	1.604	1.088	1.497	1.525
log I_{CE}	56.617	56.738	56.764	57.243
ω_s†	8.0×10^{-9}	2.7×10^{-9}	4.8×10^{-9}	5.2×10^{-9}
χ_s†	2.8×10^{-6}	1.7×10^{-6}	1.4×10^{-6}	1.9×10^{-6}
v_s (km s^{-1})†	0.138	0.075	0.094	0.123
log J_{CE}†	49.376	49.064	49.312	49.788
ω_s§	1.9×10^{-6}	5.1×10^{-7}	1.1×10^{-6}	2.6×10^{-6}
χ_s§	1.5×10^{-1}	5.8×10^{-2}	7.3×10^{-2}	4.7×10^{-1}
v_s (km s^{-1})§	32.7	13.9	21.2	61.1
log J_{CE}§	50.896	50.442	50.800	51.657

† Refers to the case of constant specific angular momentum within the red-giant convective envelope.

§ Refers to the case of solid-body rotation of the red-giant convective envelope.

In fact, they exceed the maximum angular velocities that a main-sequence star can have, a point to which we will return shortly. This result is another reflection of the fact that for solid-body rotation little angular momentum is deposited into the radiative zone as the convective envelope retreats outward. There is an indication in Table 1 that somewhat larger values of ω_{MS} might be required for Population I giants.

The present results are based on red giant sequences constructed with $l/H_p = 1$. The effective temperatures of these sequences would agree better with the observations if l/H_p were increased to about 1.5 (Cohen, Frogel, and Persson 1978). Increasing l/H_p causes a blueward shift of the red giant tracks and hence a reduction in the value of I_{CE}. Red giant sequences computed for $(M, Y, Z) = (0.90, 0.20, 0.001)$ and various values of l/H_p show that there is also a reduction in r_b (Sweigart 1979). These changes in I_{CE} and r_b nearly compensate, so the net effect on the integrand in equation (15) is fairly small. Consequently ω_{MS} should not appreciably depend on l/H_p.

Data on a number of rotation quantities have been obtained for the red giant models of Table 2 by using the values of ω_{MS} given in Table 1 for solid-body rotation. Table 2 shows that the rotation is again only a minor perturbation to the interior structure at the hydrogen, oxygen, and carbon shells ($\chi_r \approx 10^{-2}$) and at the base of the convective envelope ($\chi_r \approx 10^{-5}$–10^{-4}). However, a difficulty clearly exists at the surface where the values of χ_s are too large. Moreover, the surface rotation velocities v_s far exceed the observed upper limits for red giant stars (Kraft 1970; Strittmatter and Norris 1971). Along the RGB χ_s and v_s vary approximately as $1/R$ and thus would decrease during the subsequent evolution.

The above results demonstrate that solid-body rotation of the convective envelope leads to prohibitively large values of ω_{MS}. The fact that CNO anomalies are observed in red giant stars could be interpreted as evidence for some departure from solid-body rotation. We will now argue that such departures are physically reasonable. We first consider the question: where within the convective envelope would departures from solid-body rotation be most likely to occur? A tentative answer can be obtained by using the mixing-length theory. Assume that a convective element conserves its angular momentum while moving radially a distance of one mixing length l. When the convective element dissipates, its final angular velocity ω_f will differ from its initial angular velocity ω_i by an amount depending on l. More specifically, we have $\omega_f/\omega_i = (r_i/r_f)^2$, where r_i and r_f are the initial and final radii, respectively. Values of ω_f/ω_i have been computed for a red giant model with $(M, Y, Z) = (0.90, 0.20, 0.0001)$, $\log L = 2.31$, and $l/H_p = 1$. The results, presented in Figure 4, show that the angular velocity of a convective element can change significantly. Figure 4 implies that the convective motions lead to a substantial inward flux of angular momentum, especially in the inner part of the convective envelope. Such an inward flux would redistribute the angular momentum in a way that increases the specific angular momentum j throughout the inner part of the convective envelope. It is there that departures from solid-body rotation would be expected to be most pronounced. Increasing l/H_p to 1.5 would accentuate this redistribution. It seems plausible that the convective envelope might gradually deviate from solid-body rotation as r decreases. One might have a situation in which j is roughly constant in the inner part of the convective envelope while the outer part continues to rotate as a solid body.

It is worthwhile to point out the differences which exist between the convective envelopes of main-sequence and red giant stars. In a main-sequence star l/r is much less than 1, and thus changes in the angular velocities of the convective elements are relatively small. Moreover, the factor by which the surface radius differs from the radius at the base of the convective envelope is much less in main-sequence stars than the value of 10–100 found in red giant stars. For these reasons a red giant star would be more likely to show departures from solid-body rotation.

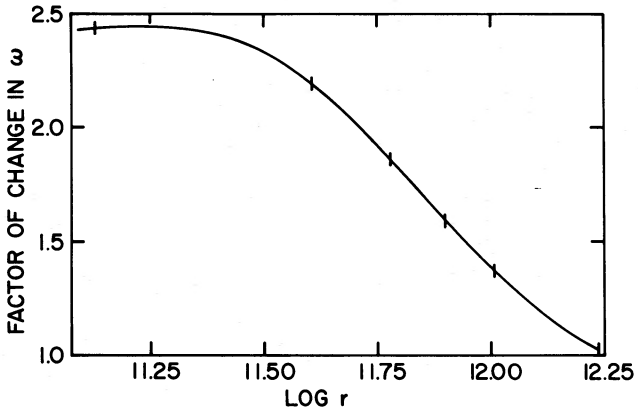

FIG. 4.—Factor by which the angular velocity ω of a convective element changes over a mixing length as a function of the radius r within the convective envelope of a red giant model with the parameters $(M, Y, Z) = (0.90, 0.20, 0.0001)$ and $\log L = 2.31$. A convective element is assumed to conserve its angular momentum while moving from its initial to final positions. Descending (rising) elements therefore experience an increase (decrease) in ω. The mixing length is taken to be 1 pressure scale height. The curve extends from the base of the convective envelope to the surface. Tick marks are separated by 0.1 $M_\odot$ in M_r and thus indicate the distribution of mass within the convective envelope.

What effects would a departure from solid-body rotation have on the present results? We consider this question for the model in Figure 4. Let us arbitrarily assume that j is constant throughout the region in which ω_f and ω_i differ by more than a factor of 2, i.e., for $\log r < 11.71$. Let us also assume that the region with $\log r > 11.71$ continues to rotate as a solid body. The amount of angular momentum that must be added to the region inside $\log r = 11.71$ to make j constant is $\sim 10\%$ of J_{CE} and hence would not significantly affect the angular velocity of the region outside $\log r = 11.71$. However, such a redistribution would increase j_b, the specific angular momentum at the base of the convective envelope ($\log r_b = 11.10$), by a factor of 17. To offset this increase in j_b, one would have to reduce ω_{MS} by a factor of 17, i.e., to a value of $\sim 10^{-4}$ rad s^{-1}, if the amount of CNO processing is to remain the same. Such a reduction in ω_{MS} would not alter the values of ω_r, χ_r, or v_{EV} given in Table 2 at the hydrogen, oxygen, and carbon shells and at the base of the convective envelope, since j_b would not have changed from its value in the case of complete solid-body rotation. However, this reduction in ω_{MS} would decrease ω_s and v_s by a factor of 17 and χ_s by a factor of 275. The predicted surface velocities would then no longer conflict with the observations.

The above considerations suggest the following points:

1. The convective motions in a red giant star might produce a departure from solid-body rotation within the inner part of the convective envelope.
2. The addition of only a small fraction of the total angular momentum into the inner part of the convective envelope would greatly increase j_b.
3. Such a redistribution of the angular momentum would greatly reduce the value of ω_{MS} required for substantial CNO processing.

There is another mechanism which could contribute to the mixing in the case of solid-body rotation. The increase in I_{CE} during the evolution up the RGB causes a decrease in ω_{CE} and hence j_b. Each mass shell as it leaves the convective envelope will therefore have a lower specific angular momentum than the preceding mass shell, thus implying that $dj/dr < 0$ within the radiative zone above the hydrogen shell. In the models of Table 2, j varies by a factor of ~ 1.5 across this zone. Since the stability conditions of the Goldreich-Schubert instability require that $dj/dr \geq 0$, mass motions in addition to the Eddington-Vogt circulation currents will be set up (Goldreich and Schubert 1967; Fricke 1968). The circulation velocity v_{GS} of the Goldreich-Schubert currents is related to v_{EV} (see eq. [13] of Endal and Sofia 1978). For the sequences in Table 1 we find that $v_{GS}/v_{EV} \approx 0.25$–1, which suggests that the Goldreich-Schubert instability may also be important in dredging up CNO-processed material. The Goldreich-Schubert instability, of course, plays no role in the constant j_{CE} case, since j is then the same everywhere in the radiative zone and the stability conditions are not violated.

In the following section we compare several aspects of the present results with the available observations.

IV. COMPARISON WITH OBSERVATIONAL DATA

a) Main-Sequence Angular Velocities

An obvious question concerns whether the values of ω_{MS} required for substantial meridional mixing are plausible. The mean angular velocities observed in main-sequence stars of intermediate mass ($M \approx 2$–$5\ M_\odot$) are $\sim 10^{-4}$ rad s^{-1} (Allen 1973). Main-sequence stars later than about F2 are known to rotate quite slowly (Kraft 1970), so for these stars the answer would appear to be no. However, the observed drop in the angular velocities around F2 might merely reflect a spin-down of the outer convective layers, and thus the interior might still be rotating (Tarafdar and Vardya 1971). Supposing this to be the case, one can extrapolate the results of Kraft (1970) to obtain the specific angular momentum in the interior of a main-sequence star later than F2. Some caution should be exercised here, since the observed angular velocities apply to field stars, and it is not known if the same statistics also hold for globular cluster stars. Assuming solid-body rotation in the interior, one can then estimate the mean angular velocity from the moment of inertia given by stellar models. For a typical globular cluster star this procedure yields $\omega_{MS} \approx 2 \times 10^{-4}$ rad s^{-1}. The spin-down of the convective envelope does not significantly affect this result, since the convective envelope of a globular cluster star is quite shallow during the main-sequence phase and thus makes only a slight contribution to the moment of inertia and the total angular momentum.

A second argument based on the morphology of the horizontal branch can be given for main-sequence angular velocities of $\sim 2 \times 10^{-4}$ rad s^{-1} and for interior rotation in red giant stars (Renzini 1977). If the interior retains its angular momentum, the contracting helium core should spin up during the ascent of the RGB. This will delay the heating of the core to the helium-ignition point, thereby resulting in a higher luminosity at the tip of the RGB (Mengel and Gross 1976). Fusi-Pecci and Renzini (1975) have argued that a range in luminosity at helium ignition of roughly $\frac{1}{8}$ mag sufficiently varies the mass lost by stellar winds to produce a dispersion of a few hundredths of a solar mass on the horizontal branch. A mass spread of this size has been invoked to explain the observed horizontal-branch morphology (Rood 1973). From the calculations of Mengel and Gross (1976), Renzini (1977) has found that a value of ω_{MS} of $\sim 2 \times 10^{-4}$ rad s^{-1} is needed to produce this range in luminosity.

Although the above arguments are not conclusive, they are at least consistent with the hypothesis that main-sequence stars later than F2 have interior angular velocities of $\sim 10^{-4}$ rad s^{-1} and that the angular momentum is retained into the red giant phase. A comparison between these expected angular velocities and those required by meridional mixing in the case of constant j_{CE} is encouragingly favorable. If constant j_{CE} describes the angular-

momentum distribution within the convective envelope, then meridional mixing might lead to substantial CNO processing of the envelope. Meridional mixing cannot be important if the convective envelope rotates completely as a solid body. However, the arguments discussed in § III*c* suggest that this difficulty can be readily overcome if the inner part of the convective envelope deviates from solid-body rotation. We conclude therefore that, as long as solid-body rotation does not continue into the base of the convective envelope, the angular velocities required by the present theory of meridional mixing should be consistent with those expected in the interior of main-sequence stars.

b) Extent of ON *Processing*

The results of § II have shown that the extent to which oxygen is involved in the CNO processing of the envelope depends on Z. The extent of ON processing probably also depends on ω_{MS}, since the circulation currents in a more rapidly rotating star would be expected to penetrate deeper into the oxygen-depleted region above the hydrogen shell. Smaller values of Z or larger values of ω_{MS} should favor a greater oxygen involvement. We now consider whether these predictions are consistent with the observations.

Whether or not the processed material being mixed into the envelope has undergone ON processing makes little difference as far as the carbon abundance of the material is concerned. It does, however, strongly influence the nitrogen abundance, since oxygen is primordially the most abundant CNO element. Carbon *et al.* (1979) have reported that the red giant stars in M92 do not show the expected anticorrelation between carbon and nitrogen. The present results would suggest the following interpretation. For the more slowly rotating stars the circulation currents might reach only into the CN-processed region above the hydrogen shell. As the angular velocity increases, the circulation currents might reach progressively deeper into the ON-processed region, and hence the nitrogen abundance of the processed material would be a function of the angular velocity. Such mixing would produce a range in the envelope nitrogen abundance for the same envelope carbon abundance. The lack of a carbon-nitrogen anticorrelation in M92 might therefore be attributable to varying amounts of ON processing due to a range in the initial angular velocity.

The field WGB stars have nearly solar [Fe/H], and hence the circulation currents would not be expected to dredge up ON-processed material. This prediction is consistent with the spectral analyses of Sneden *et al.* (1978) and Cottrell and Norris (1978), who find no evidence for oxygen depletion in two field WGB stars. The same result would also be expected if the field WGB stars are due to meridional circulation during the main-sequence phase (Cottrell and Norris 1978). The region of oxygen depletion lies very deep in a main-sequence star and should be effectively shielded from the circulation currents by a large μ gradient.

The fact that the observed spread in CN strengths is considerably larger among globular cluster giants than among Population I giants can also be understood in terms of meridional mixing. Deming (1978) has shown that CN enhancement in metal-poor stars requires ON processing if one assumes a solar C:N:O abundance ratio. In Population I stars significant ON processing would lead to a pronounced strengthening of the CN bands in contradiction to the observations (Deming 1978). CNO processing in Population I stars has probably been limited to the CN cycle. The smaller values of the C/N ratio in metal-poor field giants as compared with metal-rich field giants also imply more extensive CNO processing at low metal abundances (Sneden 1973, 1974). These differences in the size of the CN variations and in the C/N ratio agree well with the present theory of meridional mixing.

The most extreme CN-strong stars are found in ω Cen, where nitrogen enhancements by a factor of 40 have been reported by Dickens and Bell (1976). Carbon is not, however, overabundant in these extreme CN-strong stars, as shown by the absence of the C_2 Swan bands. It may be no coincidence that the largest nitrogen enhancements are found in a metal-poor globular cluster. The question of how large a nitrogen enhancement can result from CNO processing is complicated by the possibility that the primordial CNO abundances might not scale with [Fe/H] at low metal abundances. For solar [CNO/Fe], nitrogen could be enhanced by about a factor of 10. The maximum nitrogen enhancement would be particularly increased if oxygen were overabundant relative to Fe. Observational support for such an oxygen overabundance has been obtained for metal-poor field giants by Conti *et al.* (1967) and Lambert, Sneden, and Ries (1974) and for M5 by Wallerstein and Pilachowski (1978). Furthermore, the CO observations of Cohen, Frogel, and Persson (1978) and Wallerstein and Pilachowski (1978) suggest that carbon variations can exist between globular clusters of the same [Fe/H]. In view of these possible CNO variations and the uncertainties in the derived abundances, the nitrogen enhancements in ω Cen may be compatible with CNO processing alone (Dickens and Bell 1978).

The CN variations observed in metal-rich globular cluster giants are also large although less extreme than in ω Cen (Bell, Dickens, and Gustafsson 1975, 1978; Hesser, Hartwick, and McClure 1976, 1977). In such stars the circulation currents would be less likely to penetrate deeply into the oxygen-depleted region above the hydrogen shell, and thus the observations might be indicating only a partial ON processing of the envelope. In fact, ON processing might not be necessary at all if nitrogen was primordially deficient by a substantial amount in metal-rich globular clusters. A small carbon depletion would then considerably enhance the nitrogen abundance, thereby strengthening CN, and thus CN processing by itself might explain the observed CN variations. Some support for this possibility comes from the nitrogen deficiencies noted in metal-poor stars by Harmer and Pagel (1973) and Clegg (1977) and from the fact that nitrogen is a secondary element requiring the prior production of carbon and oxygen in order to be synthesized.

The CNO distributions in Figures 1–3 show that a peak in the ^{13}C abundance exists in the vicinity of the carbon shell. It is only necessary for the circulation currents to reach into this peak in order to reduce the envelope $^{12}C/^{13}C$ ratio to the low values observed in many Population I giants. ON processing is neither required nor predicted for these stars.

c) *Onset of Meridional Mixing along the RGB*

We now examine the following two questions. First, at what luminosity does the mixing of CNO-processed material into the envelope begin? Second, how suddenly along the RGB do the effects of this mixing become observable?

As discussed in § II, the present theory predicts that meridional mixing does not occur as long as there is a hydrogen discontinuity above the hydrogen shell. From evolutionary calculations it is known that the rate of evolution up the RGB slows down considerably when the hydrogen shell burns through the hydrogen discontinuity. This hesitation in the rate of evolution leads to a peak in the theoretical luminosity function (Iben 1968*a*; Rood 1972; Sweigart 1978, 1979) and in many cases to a temporary drop in the surface luminosity (Thomas 1967; Iben 1968*b*; Refsdal and Weigert 1970; Sweigart and Gross 1978). The luminosity L^* at the onset of meridional mixing (i.e., at the time when $M_{sh} = M_{sh}^*$) is tabulated in Table 3 for the red giant sequences of Sweigart and Gross (1978). We note from Table 3 and from the peaks in the luminosity functions in Figures 6 and 7 of Sweigart (1978) that L^* decreases with decreasing M or Y or increasing Z. L^* may also depend on the value of [CNO/Fe], but at the present time it is difficult to assess the importance of this dependence, since red giant sequences in which CNO is decoupled from Fe have not been computed.

The relative variation in the amount of CNO-processed material mixed into the envelope along the RGB is given by the ratio $F(M_{sh})/F(M_c)$ (see eqs. [9], [12], and [15]). The values of $F(M_{sh})/F(M_c)$ for a red giant sequence with $(M, Y, Z) = (0.90, 0.20, 0.0001)$ are plotted in Figure 5 over the range in luminosity between the onset of mixing and the helium-core flash. Both the cases of constant j_{CE} and solid-body rotation are represented. The curve for solid-body rotation would be only slightly modified if departures from solid-body rotation occurred within the inner part of the convective envelope. In the case of constant j_{CE} significant mixing continues to high luminosities, since j within the radiative zone above the hydrogen shell does not change during the evolution. In the case of solid-body rotation, however, j decreases appreciably during the evolution and therefore much of the mixing occurs at relatively low luminosities, thus explaining the sharper rise of the curve for solid-body rotation in Figure 5. As a measure of how suddenly the effects of the mixing become observable, we use the luminosity difference $\Delta \log L$ between the onset of mixing and the point where $F(M_{sh})/F(M_c) = 0.5$. For the present sequence we find that $\Delta \log L = 0.5$ and 0.15, respectively, for the cases of constant j_{CE} and solid-body rotation. These estimates for $\Delta \log L$ could actually be upper bounds if the amount of CNO processing is very extensive. As the envelope approaches CNO equilibrium, continued mixing has progressively less effect on the surface CNO abundances. A relatively small value of $F(M_{sh})/F(M_c)$ might then correspond to fairly substantial CNO processing so that the onset of the CNO anomalies would appear to be more sudden than indicated in Figure 5.

TABLE 3

LUMINOSITY AT ONSET OF MERIDIONAL MIXING

M	Y	Z	log L^*	M	Y	Z	log L^*
0.90	0.10	0.00001	2.33	0.70	0.40	0.001	2.28
0.70	0.20	0.00001	2.38	0.90	0.20	0.004	1.71
0.90	0.20	0.00001	2.49	0.70	0.30	0.004	1.78
0.70	0.30	0.00001	2.55	0.90	0.10	0.01	1.30
0.90	0.30	0.00001	2.65	1.10	0.10	0.01	1.40
0.70	0.40	0.00001	2.73	0.90	0.20	0.01	1.50
0.90	0.10	0.0001	2.12	1.10	0.20	0.01	1.61
0.70	0.20	0.0001	2.17	1.40	0.20	0.01	1.78
0.90	0.20	0.0001	2.29	1.75	0.20	0.01	1.96
1.40	0.20	0.0001	2.49	2.20	0.20	0.01	2.14
0.70	0.30	0.0001	2.35	0.70	0.30	0.01	1.57
0.90	0.30	0.0001	2.48	0.90	0.30	0.01	1.72
1.40	0.30	0.0001	2.71	1.10	0.30	0.01	1.85
0.70	0.40	0.0001	2.55	1.40	0.30	0.01	2.03
0.90	0.20	0.0004	2.14	1.75	0.30	0.01	2.23
0.70	0.30	0.0004	2.20	0.70	0.40	0.01	1.81
0.90	0.10	0.001	1.80	1.10	0.40	0.01	2.10
0.70	0.20	0.001	1.87	0.90	0.20	0.04	1.17
0.90	0.20	0.001	1.99	1.75	0.20	0.04	1.65
0.70	0.30	0.001	2.06	0.70	0.30	0.04	1.27
0.90	0.30	0.001	2.20	1.75	0.30	0.04	1.90

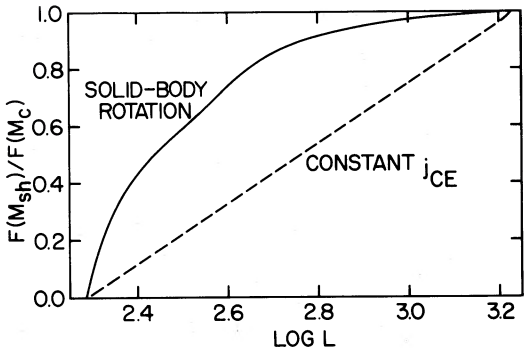

FIG. 5.—Relative variation in the amount of CNO-processed material mixed into the envelope along a red giant sequence with the parameters $(M, Y, Z) = (0.90, 0.20, 0.0001)$. The cases of constant specific angular momentum j_{CE} and of solid-body rotation within the convective envelope are represented by the dashed and solid curves, respectively. These curves extend from the onset of mixing at $\log L = 2.29$ to the helium-core flash. The ratio $F(M_{sh})/F(M_c)$ gives the amount of CNO-processed material mixed into the envelope by the time the hydrogen shell reaches the mass point M_{sh} divided by the total amount of CNO-processed material mixed into the envelope by the time of the helium-core flash.

Bell, Dickens, and Gustafsson (1978, 1979) have reported that carbon depletion among the red giant stars in M92 and NGC 6397 begins at $M_V = -0.7$ corresponding to $\log L = 2.3$. This observed luminosity for the onset of carbon depletion agrees exactly with what meridional mixing would predict if we take the parameters $(M, Y, Z) = (0.90, 0.20, 0.0001)$ to be representative of these two metal-poor globular clusters (see Table 3). According to Bessell and Norris (1976) the CN enhancements among the anomalous giants of ω Cen become noticeably more pronounced at luminosities greater than $M_V \approx -1.3$ ($\log L \approx 2.6$). Although meridional mixing would be expected to begin at a lower luminosity in ω Cen, the effects of the mixing might not become fully evident until the luminosity somewhat exceeds $\log L^*$. It appears therefore that the change in the CN enhancements along the RGB of ω Cen is also consistent with meridional mixing.

The $^{12}C/^{13}C$ ratios determined by Tomkin, Lambert, and Luck (1975) and Tomkin, Luck, and Lambert (1976) for members of the Hyades moving group show that at lower luminosities ($1.6 \leq \log L \leq 2.3$) the observed $^{12}C/^{13}C$ ratios are consistent with the normal mixing associated with the inward penetration of the convective envelope on the SGB, while at higher luminosities ($\log L \approx 2.6$) the $^{12}C/^{13}C$ ratios are too low to be explained by this normal mixing. For the estimates of the Hyades composition and turnoff mass given by van den Heuvel (1975) for a distance modulus of 3.21 mag, $\log L^*$ is roughly 2.2 ± 0.1. If we allow an interval in $\log L$ of, say, 0.3 for the meridional mixing to reduce the envelope $^{12}C/^{13}C$ ratio, we would then predict low $^{12}C/^{13}C$ ratios in giants brighter than $\log L \approx 2.5$, in good agreement with the Hyades observations.

The problem of how extensive the CNO anomalies are among faint globular cluster giants needs further observational investigation. However, the available observations indicate that some anomalous stars are too faint to be explained by the present theory (Carbon *et al.* 1979). Hesser (1978), for example, has provided tentative evidence that CN variations might persist down to the main sequence in 47 Tuc. One can, of course, appeal to primordial abundance variations to account for these faint anomalous stars. Another possibility, to be explored in the following subsection, is that these stars result from meridional mixing during the main-sequence phase.

d) Meridional Circulation during the Main-Sequence Phase

It has been frequently stated that meridional circulation does not operate in low-mass stars during the main-sequence phase due to the μ gradient created by the hydrogen burning. This statement assumes that one can determine theoretically the critical μ gradient needed to inhibit the circulation currents. Unfortunately our knowledge of meridional circulation is incomplete in several basic respects. Meridional circulation leads to a redistribution of the angular momentum, but it is not known what distribution is eventually set up. The circulation pattern is unknown. For solid-body rotation the circulation currents would move in at the equator and out at the poles. However, the circulation currents would themselves produce deviations from solid-body rotation. The circulation pattern for solid-body rotation need not exist for differential rotation. Kippenhahn (1974) has characterized the circulation pattern as one of random circulation. The velocity of the circulation currents is affected by the size of the μ gradient, which in turn is affected by the circulation currents so that meridional circulation in a region of varying composition becomes a very nonlinear process. According to Huppert and Spiegel (1977) the penetration of the circulation currents into a μ barrier may not be negligible. In view of these uncertainties it seems difficult to make a reliable statement concerning the critical μ gradient on purely theoretical grounds. An alternative approach is to use the observations to determine the extent of the meridional circulation.

A penetration of the circulation currents inside the deepest point in mass M_{DP} reached by the convective envelope on the SGB can probably be ruled out for most main-sequence stars. A number of globular clusters possess a peak in the number distribution of stars along the RGB, e.g., M4 (Lee 1977*a*) and 47 Tuc (Lee 1977*b*). If this

observed peak is identified with the peak theoretically predicted (see § IV*c*), it follows that in most red giant stars a hydrogen discontinuity is produced at the base of the convective envelope during the SGB phase and that this discontinuity is located at the same point in mass. Otherwise the peak would either not exist or would be smeared out. Efficient meridional mixing between the surface and the layers inside M_{DP} during the main-sequence phase is incompatible with this constraint for the following reasons. If the meridional circulation were efficient enough to homogenize the composition, no hydrogen discontinuity would subsequently form at M_{DP}. Although a hydrogen discontinuity might be formed inside M_{DP} at the point of deepest penetration of the circulation currents, the location of this discontinuity would be expected to depend sensitively on ω_{MS} and hence would vary from star to star. For a sample of stars the point on the RGB at which the hydrogen shell burns through this discontinuity would then cover a range in luminosity so that a well-defined peak in the RGB number distribution would no longer be observed. For a typical globular cluster star the hydrogen discontinuity at M_{DP} is roughly 0.05 in ΔX. The observed RGB number distributions therefore indicate that a μ barrier corresponding to a ΔX of ~ 0.05 is sufficient to stop the meridional circulation.

Although meridional circulation is probably restricted to the region exterior to M_{DP}, CN processing of the envelope could still take place, since the point M_{DP} lies within the region where carbon is converted to nitrogen during the main-sequence phase. The existence of faint stars with anomalous CN abundances along the SGB could be interpreted as evidence for meridional circulation between the surface and the layers just outside M_{DP} in some main-sequence stars. These stars would presumably be the fastest rotators, while stars with more normal angular velocities would not undergo meridional mixing until the RGB phase. Because of the uncertainties mentioned above, there appear to be no firm theoretical arguments which would exclude the possibility of main-sequence meridional mixing outside M_{DP}.

e) Effects of Mass Loss

In all of our computations we have ignored the possibility that mass loss might carry away much of the angular momentum of the convective envelope. Such mass loss has been previously invoked to account for the low observed upper limits on the rotation velocities of red giant stars (Kraft 1970; Strittmatter and Norris 1971). However, the present results show that the theoretically predicted rotation velocities do not conflict with the observed upper limits. For example, the rotation velocities given in Table 2 for the case of constant j_{CE} are less than the observed upper limits by nearly two orders of magnitude. The highest rotation velocities occur when the convective envelope rotates as a solid body. For $\omega_{MS} \approx 10^{-4}$ rad s^{-1} (see §§ III*c*, IV*a*), the rotation velocities given in Table 2 for solid-body rotation would be reduced by an order of magnitude and hence below the observed upper limits. The loss of angular momentum from the convective envelope is therefore not necessary to make the predictions of stellar evolution theory compatible with the observations.

Mass loss during the RGB phase takes place almost entirely near the tip of the RGB at a time when, according to Figure 5, the CNO processing is nearly complete (see Renzini 1977 and references therein). Consequently this mass loss does not greatly affect the present results. It will, however, be quite important in determining whether CNO processing continues on the AGB. In the case of constant j_{CE} the question of whether CNO processing occurs on the AGB depends on how j of the matter being lost compares with j_{CE}. In the case of solid-body rotation the mass loss would be expected to remove almost all of the angular momentum from the convective envelope, and hence CNO processing would not then continue during the subsequent evolution. As pointed out previously, the observations do not require further CNO processing after the RGB phase.

f) Comments on Assumptions and Uncertainties

The present results involve a number of assumptions and uncertainties, some of which have been described in § IV*d*. The assumptions most fundamental to our theory are (1) that the interior of a main-sequence star rotates even though the convective envelope has spun down, (2) that a star retains its interior angular momentum into the RGB phase, (3) that the estimate for the circulation velocity v_{EV} given by equation (2) is correct to order of magnitude, and (4) that the circulation pattern efficiently mixes the radiative zone above the hydrogen shell. At present there is no compelling evidence bearing on these points. However, these assumptions are neither obviously incorrect nor unreasonable. They do not conflict in any apparent way with either the available observational data or theoretical considerations.

V. CONCLUSIONS

In the present paper we have investigated the possibility that meridional circulation driven by internal rotation might lead to the mixing of CNO-processed material from the vicinity of the hydrogen shell into the envelope of a red giant star. This theory of meridional mixing has been found to be generally consistent with the available data and to be capable of explaining a number of observational results without invoking a radical departure in the physics of the stellar interior. In fact, meridional circulation must be a normal characteristic of a rotating star. It naturally explains why the extent of the mixing varies from star to star. We suggest that meridional mixing provides a reasonable framework for understanding many of the CNO anomalies shown by the WGB and CN-strong stars as well as the low $^{12}C/^{13}C$ ratios found among the field red giant stars. The present theory of meridional

mixing cannot, however, explain stars which also have an enhancement of the *s*-process elements. We do not exclude the possibility that other processes might also contribute to some of the observed CNO anomalies, e.g., meridional circulation during the main-sequence phase and primordial abundance variations.

Our main conclusions may be summarized as follows:

1. There is a region of significant extent immediately above the hydrogen shell of a red giant star within which carbon has been depleted by the CN cycle. Closer to the hydrogen shell there is a region within which oxygen has been depleted by the ON cycle. The mass extent of these carbon- and oxygen-depleted regions decreases with increasing Z.

2. The μ gradient within the carbon-depleted region is insufficient to inhibit meridional circulation for all values of Z. For low values of Z, penetration of the circulation currents into the oxygen-depleted region should also be possible, especially for the more rapidly rotating stars; hence both CN and ON processing of the envelope might occur. For large values of Z a significant μ gradient develops within the oxygen-depleted region, thereby choking off the circulation currents. CN but not ON processing of the envelope should be possible in this case.

3. Meridional circulation might lead to substantial CNO processing of the envelope provided the main-sequence angular velocity ω_{MS} is on the order of 10^{-4} rad s^{-1}. This value for ω_{MS} assumes that the specific angular momentum is constant throughout the red giant convective envelope. If the entire convective envelope rotates instead as a solid body, the value of ω_{MS} required for substantial CNO processing is prohibitively large. However, a departure of the inner part of the convective envelope from solid-body rotation, as seems physically plausible, could readily reduce the required value of ω_{MS} to $\sim 10^{-4}$ rad s^{-1}. Main-sequence stars might be reasonably expected to have interior angular velocities on the order of 10^{-4} rad s^{-1} if one attributes the observed slow rotation rates of lower main-sequence stars to a spin-down of the outer convective layers.

4. CNO processing of the envelope by meridional mixing begins on the upper subgiant branch or lower giant branch when the hydrogen shell reaches the hydrogen discontinuity produced by the convective envelope at the time of deepest penetration on the subgiant branch. The luminosity at the onset of mixing decreases with decreasing M or Y or increasing Z.

5. The WGB stars can be explained by the meridional mixing of CNO-processed material into the envelope. We attribute the lack of an observed correlation between the amounts of carbon depletion and nitrogen enhancement among the RGB stars of M92 to varying amounts of ON processing of the mixed material due to a range in the initial main-sequence angular velocity.

6. The CN-strong stars can also be understood in terms of the meridional mixing of CNO-processed material. The present results suggest that the larger CN variations observed in Population II stars might be due to more extensive ON processing of the mixed material, particularly in the case of the extreme CN-strong stars in ω Cen. For Population I compositions, ON processing of the mixed material becomes unlikely, resulting in smaller CN variations, as observed.

7. Meridional mixing could also lead to a reduction in the $^{12}C/^{13}C$ ratio if the circulation currents reached into the ^{13}C peak at the top of the carbon-depleted region above the hydrogen shell.

The authors wish to express their appreciation to R. Bell, D. Butler, D. Carbon, D. Deming, R. Dickens, A. Endal, R. Kraft, J. Laird, R. McClure, J. Norris, A. Renzini, H. Smith, S. Sofia, and W. Sparks for many stimulating discussions, for providing results prior to publication, and for clarifying many points concerning the observations. This research was carried out while one of us (A. V. S.) held a National Research Council Senior Research Associateship.

REFERENCES

Allen, C. W. 1973, *Astrophysical Quantities* (3d ed.; London: Athlone Press).
Baker, N., and Kippenhahn, R. 1959, *Zs. f. Ap.*, **48**, 140.
Bell, R. A., and Butler, D. 1979, in preparation.
Bell, R. A., Dickens, R. J., and Gustafsson, B. 1975, *Bull. AAS*, **7**, 535.
———. 1978, Symposium on Important Advances in 20th Century Astronomy, Copenhagen.
———. 1979, *Ap. J.*, **229**, 604.
Bessell, M. S., and Norris, J. 1976, *Ap. J.*, **208**, 369.
Bidelman, W. P. 1951, *Ap. J.*, **113**, 304.
Bidelman, W. P., and MacConnell, D. J. 1973, *A.J.*, **78**, 687.
Bolton, A. J. C., and Eggleton, P. P. 1973, *Astr. Ap.*, **24**, 429.
Bond, H. E. 1974, *Ap. J.*, **194**, 95.
Butler, D., Carbon, D., and Kraft, R. P. 1975, *Bull. AAS*, **7**, 239.
Butler, D., Dickens, R. J., and Epps, E. 1978, *Ap. J.*, **225**, 148.
Cannon, A. J. 1912, *Harvard Ann.*, **56**, 104.
Carbon, D., Langer, E., Butler, D., Kraft, R., Trefzger, C., Kemper, E., Suntzeff, N., and Nocar, J. 1979, in preparation.
Clayton, D. D. 1968, *Principles of Stellar Evolution and Nucleosynthesis* (New York: McGraw-Hill).
Clegg, R. E. S. 1977, *M.N.R.A.S.*, **181**, 1.
Cohen, J. G., Frogel, J. A., and Persson, S. E. 1978, *Ap. J.*, **222**, 165.
Conti, P. S., Greenstein, J. L., Spinrad, H., Wallerstein, G., and Vardya, M. S. 1967, *Ap. J.*, **148**, 105.
Cottrell, P. L., and Norris, J. 1978, *Ap. J.*, **221**, 893.
Cox, A. N., and Stewart, J. N. 1970, *Ap. J. Suppl.*, **19**, 261.
Dean, C. A., Lee, P., and O'Brien, A. 1977, *Pub. A.S.P.*, **89**, 222.
Dearborn, D. S. P., Bolton, A. J. C., and Eggleton, P. P. 1975, *M.N.R.A.S.*, **170**, 7P.
Dearborn, D. S. P., Eggleton, P. P., and Schramm, D. N. 1976, *Ap. J.*, **203**, 455.
Dearborn, D. S. P., Lambert, D. L., and Tomkin, J. 1975, *Ap. J.*, **200**, 675.
Deming, D. 1978, *Ap. J.*, **222**, 246.
Deming, D., Olson, E. C., and Yoss, K. M. 1977, *Astr. Ap.*, **57**, 417.
Dickens, R. J., and Bell, R. A. 1976, *Ap. J.*, **207**, 506.
———. 1978, private communication.
Eddington, A. S. 1925, *Observatory*, **48**, 73.
———. 1929, *M.N.R.A.S.*, **90**, 54.

Eggleton, P. P. 1967, *M.N.R.A.S.*, **135**, 243.
———. 1968, *M.N.R.A.S.*, **140**, 387.
Endal, A. S. 1976, *Bull. Astr. Soc. India*, **4**, 44.
Endal, A. S., and Sofia, S. 1978, *Ap. J.*, **220**, 279.
Faber, S. M. 1977, in *The Evolution of Galaxies and Stellar Populations*, ed. B. M. Tinsley and R. B. Larson (New Haven: Yale University Observatory), p. 157.
Fowler, W. A., Caughlan, G. R., and Zimmerman, B. A. 1975, *Ann. Rev. Astr. Ap.*, **13**, 69.
Freeman, K. C., and Rodgers, A. W. 1975, *Ap. J. (Letters)*, **201**, L71.
Fricke, K. 1968, *Zs. f. Ap.*, **68**, 317.
Fusi-Pecci, F., and Renzini, A. 1975, *Astr. Ap.*, **39**, 413.
Gabriel, M., and Noels, A. 1974, *Astr. Ap.*, **30**, 339.
Gingold, R. A. 1974, *Ap. J.*, **193**, 177.
Goldreich, P., and Schubert, G. 1967, *Ap. J.*, **150**, 571.
Greenstein, J. L., and Keenan, P. C. 1958, *Ap. J.*, **127**, 172.
Harmer, D. L., and Pagel, B. E. J. 1973, *M.N.R.A.S.*, **165**, 91.
Hartoog, M. R., Persson, S. E., and Aaronson, M. 1977, *Pub. A.S.P.*, **89**, 660.
Hesser, J. E. 1978, preprint.
Hesser, J. E., Hartwick, F. D. A., and McClure, R. D. 1976, *Ap. J. (Letters)*, **207**, L113.
———. 1977, *Ap. J. Suppl.*, **33**, 471.
Huppert, H. E., and Spiegel, E. A. 1977, *Ap. J.*, **213**, 157.
Iben, I., Jr. 1964, *Ap. J.*, **140**, 1631.
———. 1967, *Ap. J.*, **147**, 624.
———. 1968*a*, *Nature*, **220**, 143.
———. 1968*b*, *Ap. J.*, **154**, 581.
Janes, K. A. 1975, *Ap. J. Suppl.*, **29**, 161.
Keenan, P. C. 1942, *Ap. J.*, **96**, 101.
Kippenhahn, R. 1974, in *IAU Symposium 66, Late Stages of Stellar Evolution*, ed. R. J. Tayler (Dordrecht: Reidel), p. 20.
Kraft, R. P. 1970, in *Spectroscopic Astrophysics*, ed. G. H. Herbig (Berkeley: University of California Press), p. 385.
Lambert, D. L., Sneden, C., and Ries, L. M. 1974, *Ap. J.*, **188**, 97.
Lee, S.-W. 1977*a*, *Astr. Ap. Suppl.*, **27**, 367.
———. 1977*b*, *Astr. Ap. Suppl.*, **27**, 381.
Mallia, E. A. 1975, *M.N.R.A.S.*, **170**, 57P.
———. 1977, *Astr. Ap.*, **60**, 195.
McClure, R. D., and Norris, J. 1977, *Ap. J. (Letters)*, **217**, L101.
Mengel, J. G., and Gross, P. G. 1976, *Ap. Space Sci.*, **41**, 407.
Mengel, J. G., and Sweigart, A. V. 1979, in preparation.
Mestel, L. 1953, *M.N.R.A.S.*, **113**, 716.
———. 1957, *Ap. J.*, **126**, 550.
Norris, J. 1978, in *IAU Symposium 80, The HR Diagram*, ed. A. G. Davis Philip and D. S. Hayes (Dordrecht: Reidel), in press.
Norris, J., and Bessell, M. S. 1977, *Ap. J. (Letters)*, **211**, L91.
Norris, J., and Zinn, R. 1977, *Ap. J.*, **215**, 74.
Paczyński, B. 1970, *Acta Astr.*, **20**, 287.
———. 1973, *Acta Astr.*, **23**, 191.
Paczyński, B., and Tremaine, S. D. 1977, *Ap. J.*, **216**, 57.
Refsdal, S., and Weigert, A. 1970, *Astr. Ap.*, **6**, 426.
Renzini, A. 1977, in *Advanced Stages in Stellar Evolution*, Proc. 7th Advanced Course of the Swiss Society of Astronomy and Astrophysics, ed. P. Bouvier and A. Maeder (Sauverny: Geneva Observatory), p. 149.
Rood, R. T. 1972, *Ap. J.*, **177**, 681.
———. 1973, *Ap. J.*, **184**, 815.
Scalo, J. M., Despain, K. H., and Ulrich, R. K. 1975, *Ap. J.*, **196**, 805.
Scalo, J. M., and Miller, G. E. 1978, *Ap. J.*, **225**, 523.
Sneden, C. 1973, *Ap. J.*, **184**, 839.
———. 1974, *Ap. J.*, **189**, 493.
Sneden, C., and Bond, H. E. 1976, *Ap. J.*, **204**, 810.
Sneden, C., Lambert, D. L., Tomkin, J. and Peterson, R. C. 1978, *Ap. J.*, **222**, 585.
Strittmatter, P. A., and Norris, J. 1971, *Astr. Ap.*, **11**, 477.
Sweet, P. A. 1950, *M.N.R.A.S.*, **110**, 548.
Sweigart, A. V. 1973, *Astr. Ap.*, **24**, 459.
———. 1978, in *IAU Symposium 80, The HR Diagram*, ed. A. G. Davis Philip and D. S. Hayes (Dordrecht: Reidel), in press.
———. 1979, in preparation.
Sweigart, A. V., and Gross, P. G. 1978, *Ap. J. Suppl.*, **36**, 405.
Tarafdar, S. P., and Vardya, M. S. 1971, *Ap. Space Sci.*, **13**, 234.
Tayler, R. J. 1973, *M.N.R.A.S.*, **165**, 39.
Thomas, H.-C. 1967, *Zs. f. Ap.*, **67**, 420.
Tomkin, J., Lambert, D. L., and Luck, R. E. 1975, *Ap. J.*, **199**, 436.
Tomkin, J., Luck, R. E., and Lambert, D. L. 1976, *Ap. J.*, **210**, 694.
van den Heuvel, E. P. J. 1975, *Ap. J. (Letters)*, **196**, L121.
Vogt, H. 1925, *Astr. Nach.*, **223**, 229.
von Zeipel, H. 1924, *M.N.R.A.S.*, **84**, 665.
Wallerstein, G., and Greenstein, J. L. 1964, *Ap. J.*, **139**, 1163.
Wallerstein, G., and Pilachowski, C. 1978, in *IAU Symposium 80, The HR Diagram*, ed. A. G. Davis Philip and D. S. Hayes (Dordrecht: Reidel), in press.
Zinn, R. 1973, *Ap. J.*, **182**, 183.
———. 1977, *Ap. J.*, **218**, 96.

JOHN G. MENGEL: Department of Engineering and Applied Science, Yale University, New Haven, CT 06520
ALLEN V. SWEIGART: Code 681, NASA Goddard Space Flight Center, Greenbelt, MD 20771